2013 IEEE/ASME International Conference on
Advanced Intelligent Mechatronics (AIM)
Wollongong, Australia, July 9-12, 2013

Mechatronic Design of Innovative Robot Hands: Integration and Control Issues

G. Palli*, S. Pirozzi, C. Natale, G. De Maria and C. Melchiorri

***Abstract*— In this paper, an overall description of the design of an innovative robotic hand developed within the DEXMART project is discussed, with particular attention to the required sensory and actuation subsystem and their integration into the mechanical structure of the hand. The integration of the hand finger, of the sensors and the actuation is reported and the motivations leading to this particular implementation are thoroughly addressed, taking into account both the mechanical constraints and the control requirements. The finger is provided with position, force and tactile sensors and it is actuated by the twisted string actuation system purposely developed for this new robot hand. The effectiveness of the proposed design solutions is preliminary evaluated by showing the performance of the system with closed-loop finger position control.**

***Index Terms*— Actuators, Sensors, Mechatronic Design, Tendon Transmission, Robotic Hands.**

I. Introduction

Recently, a renewed interest for general purpose devices, such as anthropomorphic hands, is growing both in the industrial and research contexts. Many robot hands have been designed in the past, often trying to reproduce or enhance specific features of the human hand. Researchers have been interested in designing hands with reduced number of actuators [1], with anthropomorphic aspect [2], with high dexterity potentialities [3], with very high speed [4], or compliance [5], or many other specific aspects. Some of the robot hand prototypes developed so far possess rigid and hard structures and complicated sensori-motor systems, design solutions being mainly based on non-biologically inspired mechanics, with abundance of gears, pulleys, bearings and similar hardware. This "classical" approach leads to efficient devices yet very complex, expensive and sometimes not sufficiently reliable. For example, looking at the actuation systems of the robotic hands developed so far, they are based essentially on rotative electric motors or linear pneumatic actuators [6], usually McKibben motors [7]. Besides the higher power density with respect to electric motors, the pneumatic actuation conflicts with the integration requirements, since the valves and the compressor cannot be included into the hand structure due to their dimensions and weight. In the case of electric actuators, different types of transmission systems have been adopted: the motors can be directly placed within the fingers and the palm and connected to the joint by means of harmonic drives [8], spur and worm gears [9], [10], the motors can be placed in the forearm transmitting the mechanical power by means of flexible shafts [11] or leverages [12] or tendons routed by means of pulleys [13], [14] or sheaths [5], [15], [16], but all these solutions imply design constraints that impose a certain deviation from the biological model.

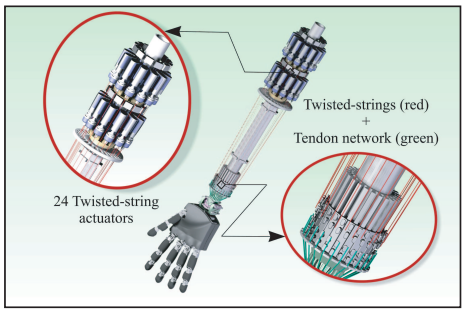

Fig. 1. The DEXMART Hand virtual prototype.

The biomimetic approach in engineering has succeeded in overcoming many difficult challenges, and this approach is increasingly applied in robotics to address problems that have proved resistant to conventional engineering solutions, as shown by the explosive growth in biomimetic research [17]. Moreover, a proper integration among mechanical parts, sensors, electronics, control algorithms, or in other words, a mechatronic approach, is one of the key concepts in the design of robotic devices in order to achieve structural simplification, increased reliability, and reduction of costs of complex devices such as robotic hands. In these systems, the problems relative to the single component or subsystem design must be solved within a general frame of compatibility and integrability. In this paper some results of the research activity carried out within the DEXMART project [18], [19] for the development of a "new generation" of robotic hands inspired by these concepts are reported. In particular, we present the main design aspects of the robotic finger, of the actuation system and of the sensing system of the DEXMART Hand characterized by: 1) a biologically-inspired endoskeletal structure; 2) an actuation system made by remotely located actuators and tendon-based transmissions routed by sliding paths; 3) an appropriate sensory apparatus that provides limited invasiveness and limitations in the design solution of the mechanical structure of the robotic hand. The paper reports a preliminary evaluation of the effectiveness of the proposed design solutions by presenting the performance of the position control loop applied to an experimental setup composed by a fully sensorized robotic finger.

II. The Mechanical Structure

The finger structure (see Fig. 2) is manufactured through 3D printing (more precisely Fused Deposition Manufac-

* Corresponding author, email: gianluca.palli@unibo.it.
Gianluca Palli and Claudio Melchiorri are with the DEI - Università di Bologna, 40136 Bologna, Italy.
Salvatore Pirozzi, Ciro Natale and Giuseppe De Maria are with the DIII - Seconda Università di Napoli, Via Roma 29, Aversa, Italy.
This research has been funded by the EC Seventh Framework Programme (FP7) under grant agreement no. 216239 as part of the IP DEXMART (DEXterous and autonomous dual-arm/hand robotic manipulation with sMART sensory-motor skills: A bridge from natural to artificial cognition).

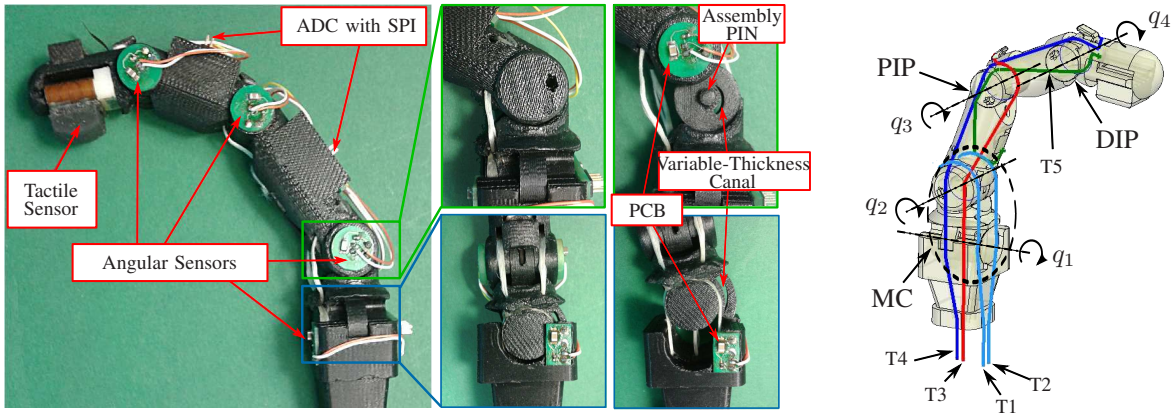

(a) Detailed view of the DEXMART Hand finger. (b) The finger tendon network.

Fig. 2. The mechanical structure of the DEXMART Hand's finger.

turing, FDM) in ABS plastic. This technique allows fast development and implementation of design alternatives with high morphological complexity. The main goal is to search for the maximum achievable integration between the finger components in the perspective of a reduction of the assembly complexity. Fingers with pin joints integrated into the phalanx body is currently the adopted solution, see Fig. 2(a), to reduce the finger assembly complexity. In spite of the sliding contacts, this solution shows very good reliability: no failures occurred after about one hundred thousand working cycles. Moreover, a deep investigation of the friction acting on the joint has been carried out and a suitable compensation algorithm has been proposed in [20].

This finger presents 4 DOFs (see the DH parameters reported in Tab. I). In particular, three identical joints have been used for the distal interphalangeal (DIP), the proximal interphalangeal (PIP) joints and the second rotational axis of the 2-DOF metacarpal (MC) joint, whereas a slightly different implementation (maintaining the same position sensor concept) has been adopted for the first rotational axis of the MC joint, see Fig. 2(a) where details of the MC joint are depicted, because of both the limited motion range of this joint and the higher mechanical strength required for this joint. Moreover, in this case the assembly pin has been removed to permit the dislocation of the joint in case of finger overload, fact that prevents damages to the mechanical structure of the finger.

Due to the quite complicated human tendon network, many different simplified solutions have been proposed in literature for the implementation of robotic hands [21]. While in the biological model the tendons slides around the bones, for the optimization of the transmission system in terms of reducing both the friction and the coupling among the hand movements, it is preferable for the tendon to traverse

TABLE I

DENAVIT-HARTENBERG PARAMETERS OF THE FINGER.

Link	d	θ [deg]	a [m]	$\alpha[rad]$
1	0	$q_1 \in [0 \ \ 40]$	$a_1 = 20.2 \cdot 10^{-3}$	$\pi/2$
2	0	$q_2 \in [0 \ \ 90]$	$a_2 = 45.0 \cdot 10^{-3}$	0
3	0	$q_3 \in [0 \ \ 110]$	$a_3 = 29.9 \cdot 10^{-3}$	0
4	0	$q_4 \in [0 \ \ 77]$	$a_4 = 21.8 \cdot 10^{-3}$	0

the endoskeleton or to be routed close to the center of rotation of the joints by means of suitable canals. The rapid prototyping manufacturing of the hand mechanical structure allows the adoption of this design solution for the tendon routing. A detailed view of the *N+1 type* tendon network of the DEXMART Hand's finger is presented in Fig. 2(b). This design choice allows minimizing the number of actuators maintaining full controllability of the joint torques. Different studies confirm that the total amount of friction acting along the tendon depends only on the friction coefficient and on the total curvature of the tendon path from the motor to the joint [22], [23], [24]. While the friction coefficient can be reduced by a suitable selection of the path coating and tendon materials (other than introducing lubricants), the path curvature minimization can be achieved by concentrating the tendon curvature in the proximity of the joint and making the path of the tendon as straight as possible between adjacent joint, as shown in Fig. 2(b). With reference to this figure, the tendons are organized as follows:

- Two tendons (T1 and T2) symmetrically disposed for the actuation of the MC joint. Thanks to the adopted configuration these tendons provide both the flexion and adduction-abduction movements;
- A flexor tendon (T3) for actuating the PIP joint having null moment arm with respect to the motion of the MC joint;
- An antagonistic tendon (T4) on the back of the finger and slides over the joints that performs extension motions;
- A coupling tendon (T5) that constrains the movements of the DIP and the PIP joints in analogy with the human hand. The path of T5 is straight to avoid contacts between the tendon and the endoskeleton and to limit friction.

Also, the selection of the tendon material plays a crucial role in tendon-based transmission. Usually, very thin steel ropes are used in tendon-based transmission systems: this approach allows to obtain a linear force-elongation behavior of the tendon but introduces some design and assembly constraints due to the limited curvature radius of steel cables. In the last years, polymeric fibers have been largely used to improve the design flexibility of tendon transmissions. Despite the comparable elastic module with respect to alloy cables, polymeric tendons present hysteresis in the force-

elongation characteristic that introduces stability problem in the transmission system control [24]. The selected tendon material is a multi-filament yarn made of Ultra High Modulus PolyEthylene (UHMPE). The capability of this commercially available polymer (Dynema® Fast-Flight) to accomplish a minimum of 100000 working cycles under different load conditions has been tested.

III. The Actuation and Sensory Apparatus

A. Actuation

Tendon-based transmission systems represent the most promising solution toward the implementation of dexterous anthropomorphic robotic hands. Taking into consideration the problems related to integration and size, rotative electric motors are nowadays the best technological solution for the actuators. Then, conversion from rotative to linear motion is needed in case of tendon-based transmission. Usually this problem is solved by means of pulleys or ballscrews connected to the motor gearbox. These solutions, even if reliable and effective, can be large and costly. Moreover, commercial miniaturized electric motors present their best efficiency at very high speed and very limited torque, a fact that implies the adoption of a gearbox with a high reduction ratio and low friction, increasing complexity, dimensions and cost of the actuation unit. To solve these problems, the so-called 'twisted string actuation system' [25], [26] has been developed. With respect to conventional solutions, the main advantages of this actuation system consist in the direct connection between the motor and the tendon without intermediate mechanisms (like gearboxes, pulleys or ball screws), in the direct transformation from rotative to linear motion, in the extremely reduced friction (only an axial bearing is needed), in the very high reduction ratio, in its intrinsic compliance and in the possibility of using very small high-speed motors. The basic concept of this actuation system is depicted in Fig. 3: the overall length of the transmission is reduced by twisting the tendons at one end by means of the motor, resulting in a linear motion of the other tendon end. A detailed analysis of this transmission system and its experimental evaluation are reported in [26]. Figure 3 also reports the scheme of the twisted string transmission system that drives the robotic finger. This actuation modality allows obtaining a very compact and lightweight actuation module as is noticeable in the CAD design of the hand prototype shown in Fig. 1 comprising 24 actuators easily located in the forearm. Moreover, in Fig. 4(a) the structure of the experimental testbed driven by four twisted string actuators adopted for the preliminary evaluation of the finger controller is shown. Note that the twisted string actuators are connected to the tendons that drive the finger via linear guides built directly into the structure of the forearm to prevent the rotation of the tendon itself. Figure 4(b) reports a detailed view of the motor module of the twisted string transmission system. This module, manufactured in ABS plastic by rapid prototyping, is characterized by an integrated force sensor (whose details will be discussed in Sec. III-B) for the implementation of the low-level force controller of the transmission system [26]. Moreover, the module is provided with a mounting rail for a

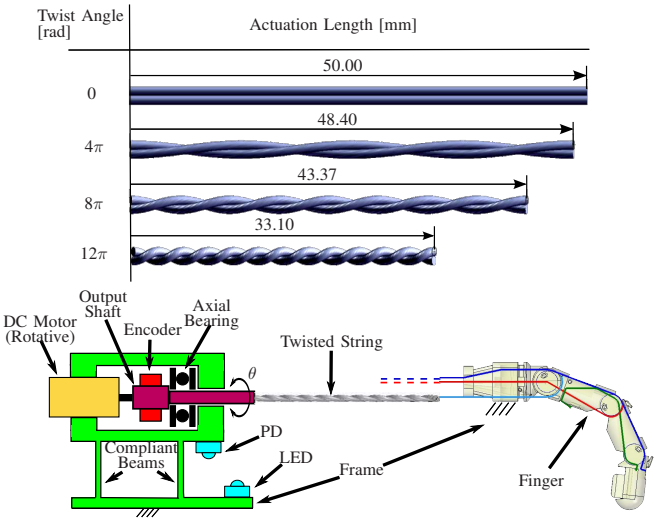

Fig. 3. Basic concept (top) and schematic representation of the twisted string actuation system (bottom).

rapid mechanical connection with the forearm structure and integrated motor power electronics, by a flexible silicon tube coupling for compensating the misalignment between the motor shaft and the transmission shaft and by an integrated combined bearing. The sensible elements of the force sensor are protected from external disturbances and from the light coming from adjacent modules by means of suitable lateral barriers. This structure has been implemented in such a way that the transmission force is entirely supported by the output shaft, the combined bearing and the flexible beams (which are necessary for the force measurement), while the motor is only used to transmit to the output shaft the necessary torque for driving the twisted string transmission system.

B. Sensors

The use of sensible elements with intrinsic high immunity to electromagnetic disturbances and with limited requirements in terms of both conditioning electronics and amplification is preferable to improve the reliability, to simplify the overall sensory subsystem and to ease its integration into a small and complex device like a robotic hand. This is the main reason why the use of commercially available optoelectronic components, LED and PhotoDetectors (PD), has been investigated for all the sensors needed in the robotic finger. All the developed sensors are based on the same principle: in non-saturation conditions, the current that flows through the PD is proportional to the light power received by the PD itself. With reference to Fig. 5 where a schematic view of the interaction between the LED and the PD is reported, since the light power P depends on both the amount and the direction of the light that flows from the LED to the PD through the relation

$$P = K \int_{\theta_1}^{\theta_2} \mathcal{I}(\theta)\mathcal{R}(\alpha + \beta - \theta)d\theta \qquad (1)$$

where K is a dimensional multiplicative constant, $\mathcal{I}(\theta)$ and $\mathcal{R}(\theta)$ the radiation pattern of the LED and the responsivity pattern of the PD respectively (available from their datasheets), it is clear that the current flowing through the

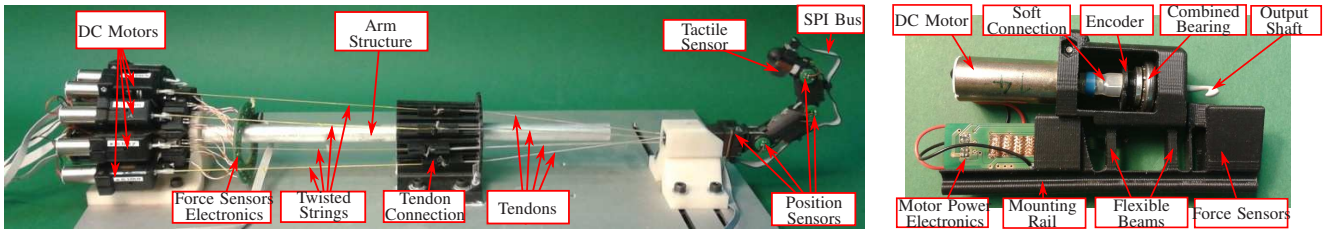

(a) Detailed view of the finger actuation module.

(b) Detail of the motor module.

Fig. 4. The finger actuation module.

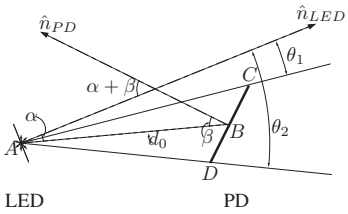

Fig. 5. Sketch of the interaction between an LED and a PD.

PD can be modulated by changing the relative position and/or orientation of the two components or by means of a mechanical part that deflects or occludes (also partially) the light that flows from the LED to the PD. This current can be measured by means of the very simple circuit reported in Fig. 6. It follows that all the sensors adopt the same condition electronics. Moreover, due to the characteristics of the optoelectronic components, it comes out that no amplifiers are necessary since the amplitude of the sensor's signal are of the same order of magnitude of the supply voltage. In particular a LED-PD couple with wide angle-of-view (HSDL-4400 and HSDL-5420 respectively, both from Avago Technologies Inc.) has been adopted for the implementation of the joint position sensors depicted in Fig. 2(a) and 8. In this sensor the LED and the PD are mounted face-to-face on one link of the joint, and the light flow is modulated by a variable-thickness canal that moves together with the joint in such a way that the PD current increase when the joint angle increase. Optoelectronic components with narrow angle-of-view (SEP8736 for the LED and the SDP8436 for the PD, both from Honeywell) have been used for the force sensor adopted for measuring the tendon force at the finger side [27], [28] and shown in Fig. 7(b). This sensor is composed by a compliant structure, made with the same material and with the same manufacturing technology used for the finger, that can be schematically represented as a flexible beam is mounted along the tendon in such a way that the tendon force cause a concentration of the load at the beam center. This load generates a deformation of the beam that can be measured by mounting the LED an the PD at the beams ends (the point of maximum angular deformation of the beam), see [29] for additional details on this sensor. The force

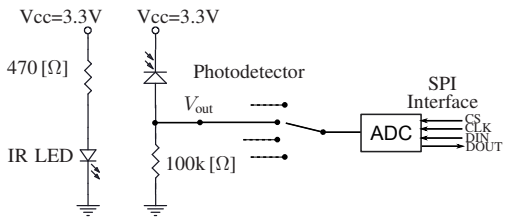

Fig. 6. Measuring circuit for the optoelectronic sensors.

sensor integrated into the motor module, see Fig. 4(b), is schematized in Fig. 7(a): the compliant structure composed by a couple of compliant beams that supports the motor produce a translation x of the upper part of the structure under the effect of the transmission force F. The behavior of the beam with constraints at both its ends highlighted by the red dashed rectangle in Fig. 7(a) is a well known topic in the field of compliant structures. Then, within the linear deformation domain, the relation between the transmission force F and the displacement x can be represented by the sum of the contribution of the two flexible beams as

$$x = \frac{F\,L^3}{24\,E\,I} \tag{2}$$

where I is the moment of inertia of the beam sectional area, L is the beam length and E is the Young's modulus of the material. The displacement x causes a variation of both the light angle and of the distance between the LED and the PD, allowing an indirect measurement of the force F through the change in the PD current caused by the deformation of the structure. A proper design of the compliant structure that supports the motor allows achieving a linear response of the sensor. Finally, many different principles can be use for the implementation of tactile sensors [30], [31], but the problem is still the integration of all the electronics and acquisition system within the limited space of the fingertip. To solve this issue, a tactile sensor based on discrete SMD optoelectronic components (SFH4050 for the LED and SFH3010 for the PD, both from OSRAM) has been developed [32], [33]. As schematized in Fig. 9(a), the working principle of this sensor is based on the reflection of the light emitted by the LED on the internal surface of a deformable layer that cover the fingertip: when a load is applied on the fingertip, the deformation of the reflecting surface cause a variation in the light path and then a variation in the current that flow through to the PD. In Fig. 9(b) the grid of 4×4 taxels (LED-PD couples) of the sensors prototype is shown. This sensor allows to directly acquire information on the deformation, due to the contact forces, of the soft pads mounted above the sensible grid without any amplification circuit. By means of a suitable calibration procedure carried out by means of a force/torque sensor and a neural network for the data processing, it is possible to reconstruct both normal and tangential forces acting on the surface of the deformable layer together with the location of the contact point. The sensor and its conditioning electronics, as depicted in Fig. 6, have been then implemented on a Rigid-Flex PCB, see Fig. 9(c), and integrated into the fingertip, as depicted in

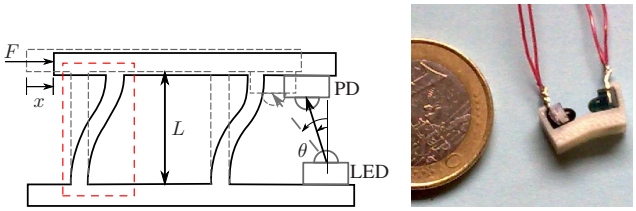

(a) Schematic view of the motor force sensor. (b) Tendon force sensors.

Fig. 7. Motor-side and finger-side force sensors.

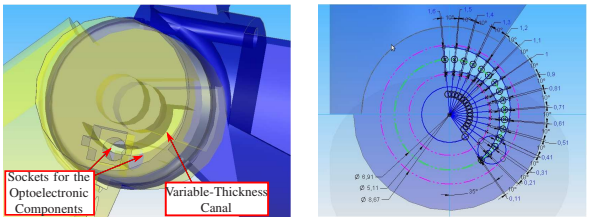

(a) Detailed view of the canal. (b) Canal dimensions (mm).

Fig. 8. Position sensors based on optoelectronic components.

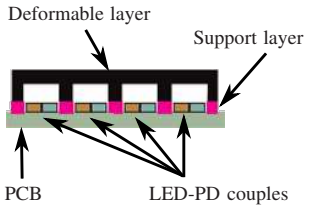

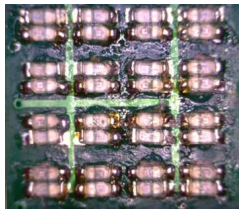

(a) Tactile sensor working principle. (b) The LED-PD grid.

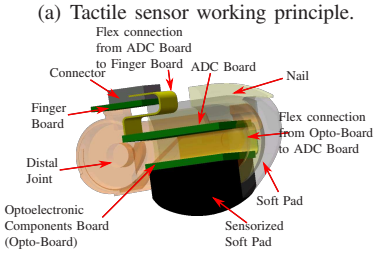

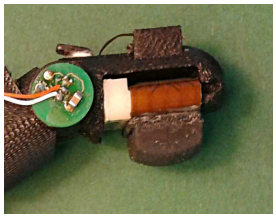

(c) Section of the fingertip with integrated tactile sensor. (d) Integration of the tactile sensor in the fingertip.

Fig. 9. Details of the tactile sensor implementation.

Fig. 9(d).

IV. Modelling and Control

Since the finger is designed in such a way that the relation between the joint angles $q = \begin{bmatrix} q_1 & q_2 & q_3 \end{bmatrix}^T$ and the displacements $l = \begin{bmatrix} l_1 & l_2 & l_3 & l_4 \end{bmatrix}^T$ of the actuated tendons (T1, T2, T3, T4) is linear, it is possible to write

$$l = H_c\, q, \qquad H_c = \begin{bmatrix} r_{11} & r_{21} & 0 \\ -r_{11} & r_{21} & 0 \\ 0 & 0 & r_{33} \\ 0 & -r_{24} & -r_{34} - \frac{r_{35}}{r_{45}} r_{44} \end{bmatrix} \tag{3}$$

where r_{ij} is the radius of the circular surface where the i-tendon envelops itself, on the j-joint. The numerical values of r_{ij} are reported in Tab. II . Note that this relation has been written considering the kinematic constraint imposed by the coupling tendon T5 that impose $q_4 = \frac{r_{35}}{r_{45}} q_3$. Due to the virtual work principle, the relation between the tendon tension f and the joint torques τ can be computed as

$$\tau = Hc^T f \tag{4}$$

The control implemented is a simple PD position control in the joint space; the desired joint torque τ_d is computed as:

$$\tau_d = K_P(q_d - q) + K_D(\dot{q}_d - \dot{q}) \tag{5}$$

where the measurement of the joint angles q are provided by the aforementioned joint position sensors and the joint velocities $\dot{q}$ are computed through suitable digital filters. In order to compute the actuation forces f_d given the desired torques τ_d, the pseudo-inverse $H_c^{T^+}$ of the coupling matrix is used:

$$\hat{f}_d = H_c^{T^+} \tau_d \tag{6a}$$

$$f_d = \hat{f}_d + \lambda f_k \tag{6b}$$

where $\hat{f}_d$ is the minimum module force vector so that $\tau_d = H_c^T \hat{f}_d$, f_k is a base of the null space of H_c^T, and $\lambda \in \mathbb{R}$ is chosen in order to impose the tendon tensions above a certain threshold f_0

$$\lambda = \max_{i \in \{1,\cdots,4\}} \frac{f_{0_i} - \hat{f}_{d_i}}{f_{k_i}} \tag{7}$$

Then, the low-level controller of the twisted actuation system applies the desired force to each tendon as described in detail in [26]. Figure 10(a) reports the results of an experiment where all joints move on their whole range and with periodic reference signals with a frequency of 0.2 Hz, whereas Fig. 10(b) shows a similar experiment at a frequency of 0.5 Hz. These particular tests were selected because they are the typical motion velocities during grasps and manipulation activities. In the reported experiments, the joint position errors are limited to few degrees, mostly because of the friction acting both on the finger joints and on the tendons (since the tendons slide in dedicated channels built within the finger itself without any mechanism for friction reduction, also in this case for achieving the maximum design simplification). These side effects can be significantly reduced by applying suitable compensation techniques, as reported in [20] for what related to the joint friction and in [24] concerning the tendon friction, and the implementation of these compensation algorithms in the finger controller will be subject of future evaluation.

V. Conclusions and Future Work

The design of a highly integrated mechatronic system like a robotic hand necessitates a sensory system that must cope with the limits of weight, encumbrance and functionality of this specific application. Moreover, where actuators and sensors that can be directly integrated and used in anthropomorphic hands do not exist on the market, suitable solutions must be investigated. Innovative approaches based on non-conventional solutions and on the study of the biological model can significantly simplify the design, enhance the reliability and the performance, reduce the costs of robotic hands. The integration of position, force and tactile sensors and of the twisted string actuation system into the hand structure is reported in this paper together with the preliminary

TABLE II

Radii of the finger circular surfaces.

	r_{11}	r_{21}	r_{33}	r_{24}	r_{34}	r_{44}	r_{35}	r_{45}
radius [mm]	8.2	7.8	6.3	5.3	5.3	5.3	3.5	5.0

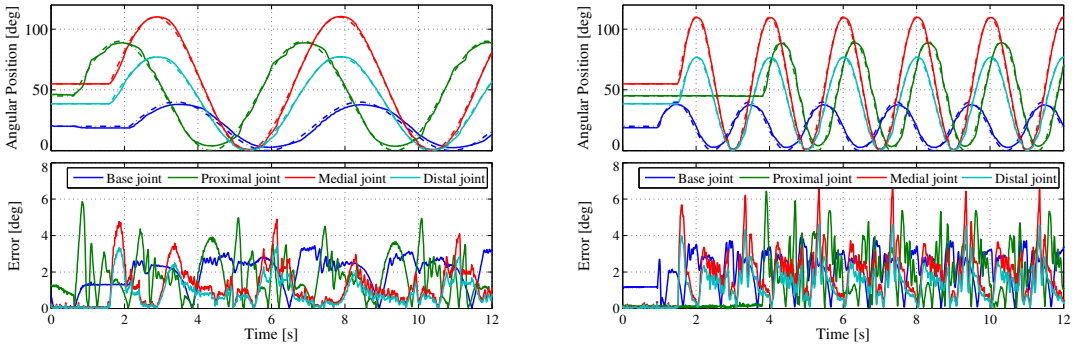

(a) Position control at 0.2 Hz. (b) Position control at 0.5 Hz.

Fig. 10. Finger position control: reference and actual signals (dash-dot and solid lines respectively in top figure) and the absolute tracking errors.

evaluation of the basic finger control functionality by means of a joint position controller.

REFERENCES

[1] L. Birglen, T. Laliberté, and C. Gosselin, *Underactuated Robotic Hands*, ser. Springer Tracts in Advanced Robotics, O. Khatib, V. Kumar, and G. Pappas, Eds. Springer Berlin / Heidelberg, 2008, vol. 40.

[2] M. Carrozza, G. Cappiello, G. Stellin, F. Zaccone, F. Vecchi, S. Micera, and P. Dario, "A cosmetic prosthetic hand with tendon driven underactuated mechanism and compliant joints: Ongoing research and preliminary results," in *Proc. IEEE Int. Conf. on Robotics and Automation*, Barcelona, Spain, 2005, pp. 2661 – 2666.

[3] H. Liu, P. Meusel, G. Hirzinger, M. Jin, Y. Liu, and Z. Xie, "The modular multisensory DLR-HIT-Hand: Hardware and software architecture," *IEEE/ASME Trans. on Mechatronics*, vol. 13, no. 4, pp. 461–469, 2008.

[4] A. Namiki, Y. Imai, M. Ishikawa, and M. Kaneko, "Development of a high-speed multifingered hand system and its application to catching," in *Proc. Int. Conf. on Intelligent Robots and Systems*, 2003, pp. 2666–2671.

[5] L. Biagiotti, F. Lotti, C. Melchiorri, G. Palli, P. Tiezzi, and G. Vassura, "Development of UB Hand 3: Early results," in *Proc. IEEE Int. Conf. on Robotics and Automation*, Barcelona, Spain, 2005, pp. 4488–4493.

[6] Shadow Robot Company, "Design of a Dextrous Hand for advanced CLAWAR applications," in *Climbing and Walking Robots and the Supporting Technologies for Mobile Machines*, Catania, Italy, 2003, pp. 691–698.

[7] P. C. Chou and B. Hannaford, "Measurement and modeling of McKibben pneumatic artificial muscles," *IEEE Trans. on Robotics and Automation*, vol. 12, no. 1, pp. 90–102, Feb. 1996.

[8] J. Butterfass, M. Grebenstein, H. Liu, and G. Hirzinger, "DLR-Hand II: Next generation of a dextrous robot hand," in *Proc. IEEE Int. Conf. on Robotics and Automation*, 2001.

[9] H. Kawasaki, T. Komatsu, and K. Uchiyama, "Dexterous anthropomorphic robot hand with distributed tactile sensor: Gifu hand II," *IEEE/ASME Trans. on Mechatronics*, vol. 7, no. 3, pp. 296–303, 2002.

[10] W. T. Townsend, "The BarrettHand Grasper Programmably Flexible Part Handling and Assembly," *Industrial Robot*, vol. 27, no. 3, pp. 181–188, 2000.

[11] C. Lovchik and M. Diftler, "The robonaut hand: a dexterous robot hand for space," in *Proc. IEEE Int. Conf. on Robotics and Automation*, 1999.

[12] N. Fukaya, S. Toyama, T. Asfour, and R. Dillmann, "Design of the TUAT/Karlsruhe humanoid hand," in *Proc. IEEE/RSJ Int. Conf. on Intelligent Robots and Systems*, 2000, pp. 13–19.

[13] K. Salisbury and B. Roth, "Kinematics and force analysis of articulated mechanical hands," in *Journal of Mechanims, Transmissions and Actuation in Design*, 1983.

[14] M. Grebenstein et al., "The DLR hand arm system," in *Proc. IEEE Int. Conf. on Robotics and Automation*, Shanghai, China, 2011, pp. 357–362.

[15] A. Caffaz, G. Cannata, G. Panin, and E. Massucco, "The DIST-hand, an anthropomorphic, fully sensorized dextrous gripper," in *In First IEEE-RAS Int. Conf. on Humanoid Robots*, 2000.

[16] G. Berselli, G. Borghesan, M. Brandi, C. Melchiorri, C. Natale, G. Palli, S. Pirozzi, and G. Vassura, "Integrated mechatronic design for a new generation of robotic hands," in *Proc. IFAC Symp. on Robot Control*, vol. 9, Part 1, Gifu, Japan, 2009, pp. 105–110.

[17] N. F. Lepora, P. F. Verschure, and T. J. Prescott, "The state-of-the-art in biomimetics," in *Biomimetic and Biohybrid Systems*, ser. Lecture Notes in Computer Science. Springer Berlin Heidelberg, 2012, vol. 7375, pp. 367–368.

[18] L. Villani, V. Lippiello, F. Ruggiero, F. Ficuciello, B. Siciliano, and G. Palli, "Grasping and control of multifingered hands," in *In Advanced Bimanual Manipulation*, B. Siciliano (Ed.), Springer Tracts in Advanced Robotics, vol. 80, Springer, 2012, pp. 219–266.

[19] G. Palli, C. Melchiorri, G. Vassura, G. Berselli, S. Pirozzi, C. Natale, G. De Maria, and C. May, "Innovative technologies for the next generation of robotic hands," in *Advanced Bimanual Manipulation*, B. Siciliano (Ed.), Springer Tracts in Advanced Robotics, vol. 80, Springer, 2012, pp. 173–218.

[20] G. Borghesan, G. Palli, and C. Melchiorri, "Friction compensation and virtual force sensing for robotic hands," in *Proc. IEEE Int. Conf. on Robotics and Automation*, Shanghai, China, 2011, pp. 4756–4761.

[21] A. Morecki, Z. Busko, H. Gasztold, and K. Jaworek, "Synthesis and Control of the Anthropomorphic Two-Handed Manipulator," in *Proc. Int. Symp. on Industrial Robotics*, Milan, Italy, 1980, pp. 461–474.

[22] M. Kaneko, M. Wada, H. Maekawa, and K. Tanie, "A new consideration on tendon-tension control system of robot hands," in *Proc. IEEE Int. Conf. on Robotics and Automation*, vol. 2, Sacramento, CA, 1991, pp. 1028–1033.

[23] G. Palli and C. Melchiorri, "Optimal control of tendon-sheath transmission systems," in *Proc. IFAC Symp. on Robot Control*, vol. 8, Bologna, Italy, 2006, pp. 73–78.

[24] G. Palli, G. Borghesan, and C. Melchiorri, "Modeling, identification and control of tendon-based actuation systems," *IEEE Trans. on Robotics*, vol. 28, no. 2, pp. 277–290, 2012.

[25] T. Würtz, C. May, B. Holz, C. Natale, G. Palli, and C. Melchiorri, "The twisted string actuation system: Modeling and control," in *Proc. Int. Conf. on Advanced Intelligent Mechatronics*, Montreal, Canada, 2010, pp. 1215–1220.

[26] G. Palli, C. Natale, C. May, C. Melchiorri, and T. Würtz, "Modeling and control of the twisted string actuation system," *IEEE/ASME Trans. on Mechatronics*, vol. 18, no. 2, pp. 664–673, 2013.

[27] G. Palli and S. Pirozzi, "Force sensor based on discrete optoelectronic components and compliant frames," *Sensors and Actuators A: Physical*, vol. 165, pp. 239–249, 2011.

[28] ——, "Miniaturized optical-based force sensors for tendon-driven robots," in *Proc. Int. Conf. on Robotics and Automation*, Shanghai, China, 2011, pp. 5344–5349.

[29] ——, "A miniaturized optical force sensor for tendon-driven mechatronic systems: Design and experimental evaluation," *Mechatronics*, vol. 22, no. 8, pp. 1097–1111, 2012.

[30] M. H. Lee and H. R. Nicholls, "Tactile sensing for mechatronics – a state of the art survey," *Mechatronics*, vol. 9, no. 1, pp. 1–31, 1999.

[31] M. E. H. Eltaib and J. R. Hewit, "Tactile sensing technology for minimal access surgery–a review," *Mechatronics*, vol. 13, no. 10, pp. 1163–1177, 2003.

[32] A. D'Amore, G. De Maria, L. Grassia, C. Natale, and S. Pirozzi, "Silicone-rubber-based tactile sensors for the measurement of normal and tangential components of the contact force," *Journal of Applied Polymer Science*, vol. 122, no. 6, pp. 3757–3769, 2011.

[33] G. De Maria, C. Natale, and S. Pirozzi, "Force/tactile sensor for robotic applications," *Sensors and Actuators A: Physical*, vol. 175, pp. 60 – 72, 2012.